

The influence of the gap diameter on the polymer thread temperature and velocity at the exit of the 3D printer nozzle

Alberto Baeza-Campuzano¹⁾ (ORCID ID: 0000-0002-7241-6836), Javier Morales-Castillo²⁾, Víctor M. Castaño^{1), *} (000-0002-2983-5293)

DOI: <https://doi.org/10.14314/polimery.2022.7.6>

Abstract: Using the example of acrylonitrile-butadiene-styrene (ABS) copolymer, the effect of the gap (thread) diameter for five printing velocity at 230°C on the thread temperature and velocity at the nozzle exit was investigated using the ANSYS Fluent simulation program. It was shown that the change of the gap diameter had a significant impact on the tested parameters.

Keywords: 3D-printing, gap diameter, effect of temperature, printing velocity.

Wpływ średnicy szczeliny na temperaturę i prędkość nici polimerowej na wyjściu z dyszy drukarki 3D

Abstrakt: Na przykładzie kopolimeru akrylonitryl-butadien-styren (ABS), za pomocą programu symulacyjnego ANSYS Fluent, zbadano wpływ średnicy szczeliny dla pięciu prędkości drukowania w temperaturze 230°C na temperaturę i prędkość nici na wyjściu z dyszy. Wykazano, że zmiana średnicy szczeliny miała istotny wpływ na badane parametry.

Słowa kluczowe: druk 3D, średnica szczeliny, wpływ temperatury, prędkość drukowania.

Fused deposition modelling (FDM) process creates a 3D printed part layer by layer. The most commonly used system is presented in Figure 1. However, not all of the systems are the same as the one presented in Figure 1. The filament and the printer head move at velocity imposed by the user, then the filament gets in contact with the heated block, the polymer filament melts and flows out of the nozzle tip with 0.4 mm diameters. This thread gets in contact with the heated bed for deposition, shearing and cooling.

Rheological properties have great influence on the mechanical properties and performance of the final printed part. For example, temperature of the bed and nozzle tip generate drastic changes in the temperature of the thread and it deposited velocity. Such phenomena occur due to high or low viscosity. Parameters and rheological properties within the 3D printer are difficult to solve and correlate, however, a series of prediction can be achieved by doing modelling. Currently existing articles explain how the 3D printed system works, describe most common problems and advise how to solved them [1, 2].

When the polymer reaches the melting state, the deposition is carried onto the printing bed, usually the printing thread is about 0.4 mm, however, in other cases, the thread might be lowered till 0.1 mm. The temperature and velocity of the thread highly depend on the feeding velocity and shearing rate, specially this last [phenomena] phenomenon is intrinsically carried out by the printing velocity. The set velocity, temperature and thread diameter, also called gap, are crucial parameters mainly because they are highly related with the viscosity. Therefore, those

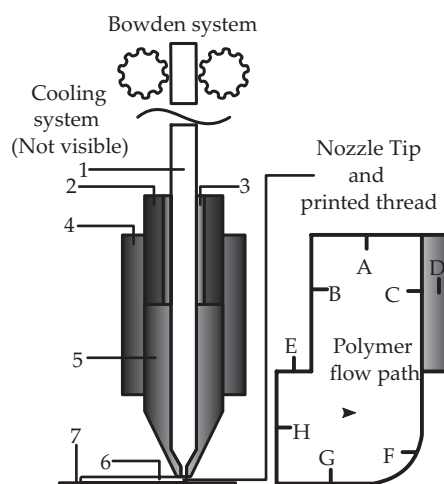


Fig. 1. Bowden system for common used 3D printers, 1) filament, 2) heat break, 3) Teflon tube guiding tube PTFE (Teflon tube), 4) heat block, 5) nozzle, 6) printed thread, 7) printing bed

¹⁾ Universidad Nacional Autónoma de México, Centro de Física Aplicada y Tecnología Avanzada, Boulevard Juriquilla 3001, Querétaro 76230, México.

²⁾ Universidad Autónoma de Nuevo León, 66420 Monterrey, Nuevo León, México.

^{*} Author for correspondence: vmcastano@unam.mx

parameters are difficult to measure doing experimental characterization. Hence, this prompts us to perform simulations to predict results and behaviors.

Many researchers are devoted to developing a fully computationally system to analyse and characterize the materials. However, not all of them consider the real cases scenarios, because of the assumptions to simplify the problem. Analysing the temperature of the thread being printed, without consideration of the shearing effect of the nozzle and the thread reduction is another problem. The parameters, variables and behaviors to consider are: Different temperatures changes due to cooling from the room temperature. The system is considered as layer by layer and the cooling process begins on all areas and surfaces of the entire thread, temperature of the printing bed is an important parameter, as well as the shearing effect between the nozzle and the bed, and the thread diameter (gap). Already exists a fully three-dimensional thermal model of FDM describing the nonlinearity effect of the deposition, developed on ANSYS finite element method [3].

Also, exist a series of tools for thermal analysis used to obtain the melt front location considering the liquefier that is governed by two dimensional axisymmetric steady-state advection-conduction equation. The heat applied onto the heat block is considered the same as applying the heat straight to the walls of the nozzle and heat break. Therefore, the flowing pattern of the melt is considered as a plug flow (constant flow during the entire cross section) [4]. However, currently there is no research in the temperature of the thread and the impact of the thread size (gap).

ANSYS polyflow have been used to simulate fiber composites flowing through the nozzle with isothermal considerations [5]. The calculation of the pressure drop while changing the nozzle degree contraction angle was carried out considering isothermal process as well [6], [7]. The nozzle tip has a great impact on temperature of the thread. There is an analysis considering the shape of the nozzle. This lead the system to a different outcome in temperature and velocity of the printing thread [8]. Also, considering thermal effects limits the attainable extrusion velocity since the maximum heat flow between filament and wall may not be high enough to fully heat the filament to the temperature set point within the nozzle tip [9]. Though in the nozzle tip the temperature only increases along the length, it does not mean that all filament is on molten state. Hence, the thread at the nozzle exit will present molten state at the wall while solid state in the center of the filament. In other words high temperatures at the wall of the filament, lowering temperature in radial direction, [it means] mean changes in velocities and pressures [10].

There are several investigations that involve the FDM technology process but few of the research considers the printing velocity achieved by the printing head. Currently there is not research considering the shear velocity applied between the printer head and the printing bed along with the changes in the thread diameter. The aim of this paper, is to show the effect of the thread size (gap) and

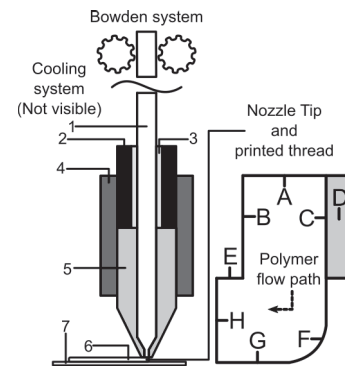


Fig. 2. Nozzle tip and thread coming out of the nozzle (system applied into fluent). A) nozzle tip entrance, B) nozzle tip left wall, C) nozzle tip right wall D) nozzle tip, E) nozzle shearing wall against the printing bed, F) right free surface of the thread coming out of the nozzle, G) printing bed, H) thread diameter varies from 0.4 mm to 0.1 mm

the printing velocity on the temperature and flow velocity of thread coming out exactly at the exit of the nozzle.

The analysis was carried out considering the nozzle tip, the thread coming out right at the exit of the nozzle entering in contact with the printing bed and the thread diameter, is it can be seen in Figure 2. ABS polymer was considered (data taken from the literature).

EXPERIMENTAL PART

Materials

One grade of acrylonitrile-butadiene- styrene copolymer (ABS) for 3D printing was used. We focused on one ABS grade but changing the gap (thread diameter). The polymer used was obtained from Mackay [11].

Rheology

The rheology was conducted as follows: Mackay, used 8 mm parallel plates, within the linear viscoelastic regime and frequency sweep range from 100 to 0.01 rad/s, at the temperatures from 210 to 250 every 10°C. The processing temperature was 230°C [11]. Power law was used to fit the polymer data. This can be seen in next sections.

Chosen velocities

During the simulation the velocity used for feeding and printing is intrinsically obtained setting the printing velocity, see equation 1 [12]

$$\frac{V_x}{V_a} = \left(\frac{D}{d'} \right)^2 \quad (1)$$

where: d' – the thread diameter (0.40 mm), D – the filament diameter (1.75 mm), V_a – printing velocity (PV), V_x – feeding velocity (FV). Equation 1 fits the most

common used 3D printers in the current market. The printing velocities proposed are 0.005 m/s as a lower extreme (rarely used). It is followed by 0.020, 0.030, 0.040, and 0.060, as the common printing velocity used. This can be seen in Table 1.

Table 1. Printing and feeding velocity applied into the simulation

Sample	Printing velocity m/s	Feeding velocity m/s
PV 1	0.005	0.000261224
PV 2	0.020	0.001040000
PV 3	0.030	0.001570000
PV 4	0.040	0.002090000
Vel 5	0.050	0.003130000

Gap-dependent (shear rate), $\dot{\gamma}$.

The thread diameter also called gap between the nozzle and printing nozzle lead us to a different analysis. When the gap decreases high shear rates are obtained along with different temperatures and velocities fields. The shear rate for different gaps and printing velocities is obtained using Equation 2 [13], [14]

$$\dot{\gamma} = \frac{U}{h} \tag{2}$$

where: U – velocity (printing velocity), h – the thread diameter or gap. Therefore, the printing velocities from table 1 and three gap diameter 0.40 mm, 0.35 mm and 0.30 mm were used.

Positions for temperatures and velocities measurement

The temperature and velocity field were obtained in one relevant position within in the system, basically where the polymer gets in contact with the printing bed and environment temperature. This can be seen in Fig. 3.

Governing equations, and boundary conditions

The temperature field of the polymer, is obtained using the governing equations like conservation of mass, con-

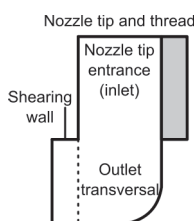


Fig. 3. Outlet transversal 1 (the material is shared by the nozzle; the thread faces are cooled by ambient temperature)

servation of momentum and conservation of energy, however, they need assumptions and boundary conditions. Considering the power law in viscosity using, Arrhenius model is used as well.

The mass conservation equation is given by Equation 3.

$$\frac{\delta u}{\delta x} + \frac{\delta v}{\delta y} = 0 \tag{3}$$

$$\rho \left(u \frac{\delta u}{\delta x} + v \frac{\delta v}{\delta y} \right) = \frac{-\delta p}{\delta x} + \mu \nabla^2 u \tag{4}$$

The first term is due to stretching in the x direction and the second term is due to stretching in the second direction. The equation of momentum conservation is shown in Equations 4 and 5.

$$\rho \left(u \frac{\delta v}{\delta x} + v \frac{\delta v}{\delta y} \right) = \frac{-\delta p}{\delta y} + \mu \nabla^2 v \tag{5}$$

Equations 4 and 5, where the first line is the momentum conservation in the x direction and the terms in the right side represent the force in the x direction for infinitesimal fluid particle. On the left side, the mass times acceleration is shown, the term $v \frac{\delta v}{\delta y}$ represents the acceleration in the x direction due to particle motion in y direction assuming steady flow and constant flow. μ represents the viscosity. It is obtained with power law fluid and the Arrhenius model. This can be observed in Equation 5.

$$\eta = K \dot{\gamma}^{n-1} H(T) \tag{6}$$

$$H(T) = \exp \left(\alpha \left(\frac{1}{T - T_0} - \frac{1}{T_\alpha - T_0} \right) \right) \tag{7}$$

Equations 6 and 7 show the viscosity as a temperature dependant where alpha is the activation energy and T_α is a reference temperature for which $H(T) = 1$. T_0 which is the temperature shift, is set to 0 by default, and corresponds to the lowest temperature that is thermodynamically acceptable. Therefore, T_α and T_0 are absolute temperatures. Temperature dependence is only included when the energy equation is enabled.

It should be noticed that in equation 5 viscosity depends on the shear rate as well, κ is the consistency index, n is a fitting parameter.

As it was mentioned before if the material depends on temperature and the Arrhenius Equations is presented, energy equation must be activated as well

$$\frac{\delta(\rho E)}{\delta t} + \nabla \cdot (\vec{V}(\rho E + p)) = \nabla \cdot [k_{\text{eff}} \nabla T - \sum_j h_j \vec{J}_j + (\vec{\tau}_{\text{eff}} \cdot \vec{V}) + S_h] \tag{8}$$

$$E = h - \frac{p}{\rho} + \frac{v^2}{2} \quad (9)$$

In Equation 8 and 9, k_{eff} is the effective conductivity. On the left side of the equation the convection term is present and the right side shows the energy transfer due to conduction, species diffusion and viscous dissipation respectively. The term S_h is heat caused by chemical reaction, which in this case is neglected. For energy we have h , that represents enthalpy, p pressure and ρ density.

Those equations were carried out with following boundary conditions:

At the entrance we have the inlet flow.

The temperature applied on the block is the same as applied directly on the heat break and nozzle

Velocity at the wall is zero.

Viscous heating is considered.

The components of the system are in perfect contact with each other.

RESULTS AND DISCUSSION

The velocity applied into the simulation was calculated with Equation 1. Figure 4 shows how the feeding velocity is obtained.

Figure 4 shows the feeding velocity obtained with equation 1. The curve presents the most common, used and commercial 3D printer. If the printing curve increases the feeding velocity increases linearly as well. However, in the real case all feeding and printing motors have a threshold. It means that at certain point the graph will not show linearity anymore, because the motor will reach its limit.

The viscosity was model with the power law function (Equation 5). This can be seen in Figure 5.

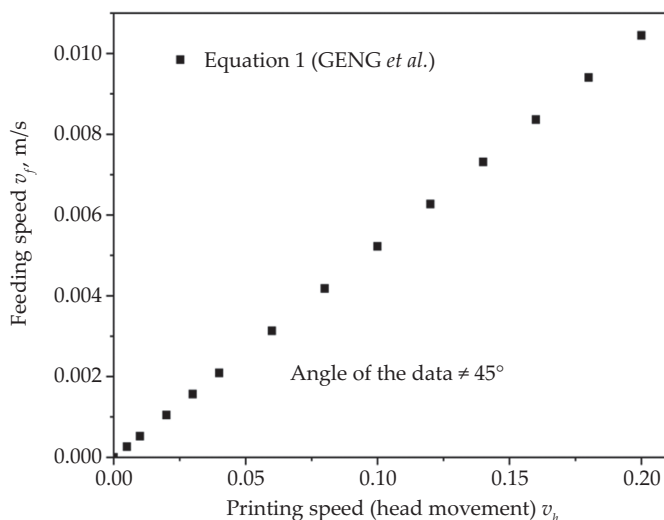


Fig. 4. Feeding velocity obtained from Equation 1, the data does not present 45° angle

Table 2. Fitting values of the powerlaw model on ABS polymers

Polymer	K	n
ABS Mackay	10239.70	0.504

As it was mentioned before the simulations were carried out in ANSYS Fluent, academic version. The location previously explained in Figure 3 is represented in Figure 6.

The results from the simulations applying 230°C, the five different velocities and three thread diameters (gap) previously mentioned, can be seen in Figure 7.

It is possible to observe in Figure 7 how the temperature decreases considerably while the feeding velocity increases. However, it is possible to see how the velocity and temperature changes when the gap increases from 0.30 mm to 0.35 mm and 0.40 mm. When the velocity field presents vortices the temperature field lowers at that point. The 0.30 mm gap presents high vortices but most of them are close to the printing bed. Hence, looking at the 0.35 mm gap it can be seen that the vortices are reduced and great impact on the temperature is present. Finally, when the gap goes to 0.40 mm the vortices are very distinct and low temperatures are predominant within the system.

Looking at the velocity 1 and 2, the system of 0.30 mm looks the most stable compared to the other two gaps. However, going further to velocity 3 and 4 the gap of 0.35 mm is the most suitable and stable, the vortices are reduced drastically, and low temperatures almost vanished. Finally, velocity 5 almost ties with 0.30 mm gap. Also, it is possible to observe that 0.40 mm presents the most instable system, having very distinct vortices and drastic temperatures changes.

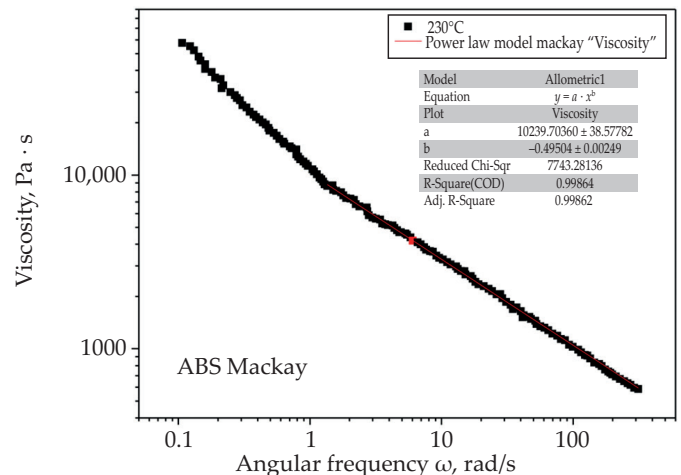


Fig. 5. Viscosity curve along with the power law model, data extracted from the author previously mentioned [11]

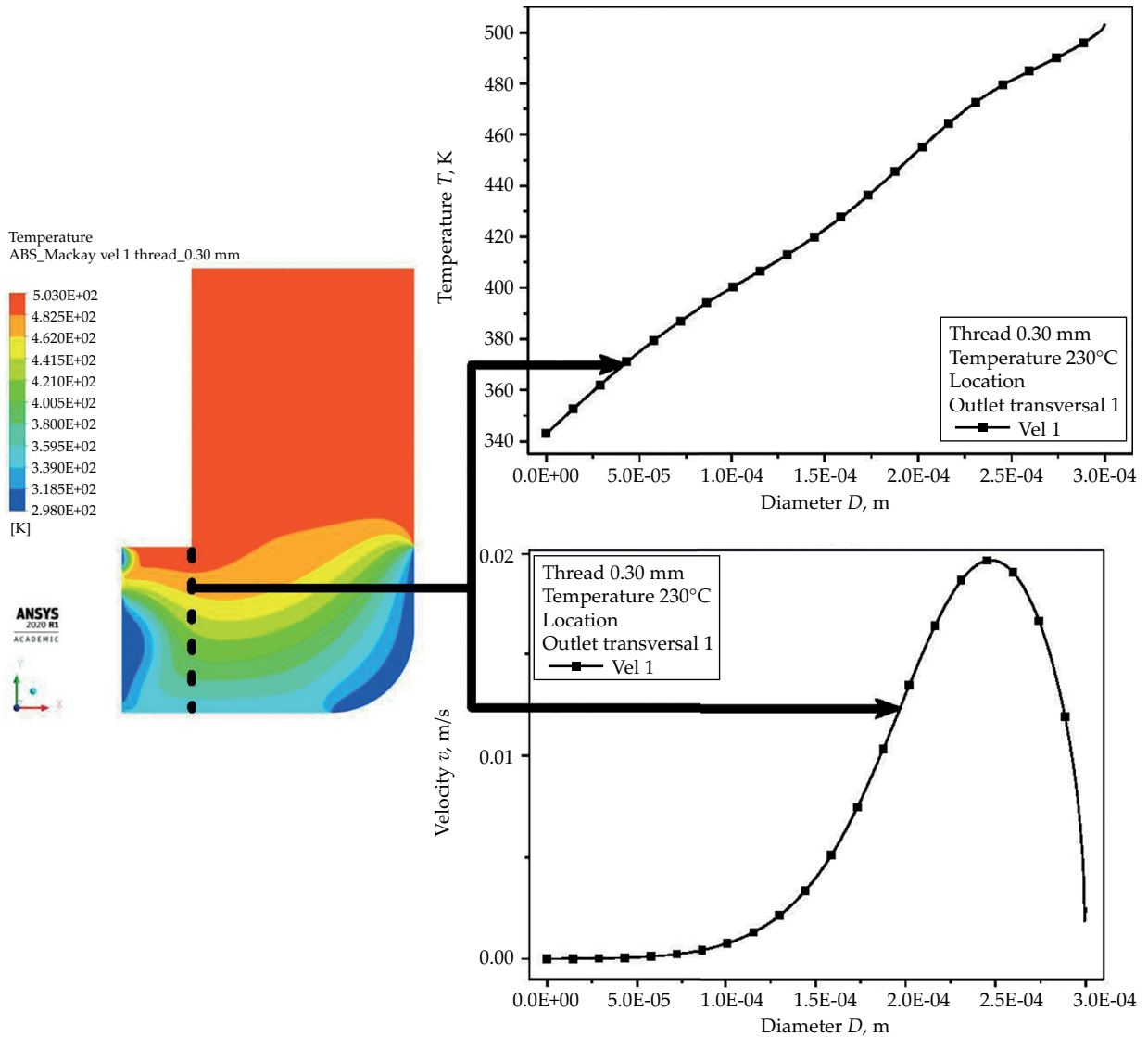


Fig. 6. The temperature and velocity behavior on the position within the system

The previously mentioned information is present in next graphs.

Figure 8 shows the temperature behavior for the three gaps. It can be seen that curves with solid line have the most stable temperatures, while the others presents instabilities with high ups and downs.

While the velocity increases the temperature behaves differently from 0.3 mm to 0.35 mm and 0.4 mm gap. The temperature at 0.35 mm gap presents better results compared to the other two. The curve at 0.35 mm gap tries to reach a threshold around 440°C after passing the overshoot and finally increases linearly (see Figure 9).

When the velocity is increased, it is possible to observe the instabilities at gap 0.40 mm (see Fig. 9b).

Figure 10 shows the correlation between the velocity and the temperatures. It is possible to observe that the velocity increases while the temperature increases as well but when the velocity reaches the highest point the temperature tries to stabilize. When the velocity decreases we can see that the temperature increases as well.

When the velocity tries to stabilize at certain value, the temperature tries to stabilize as well, but when the velocity values are fluctuating without possible stabilization the temperature does the same. Also, if the temperature

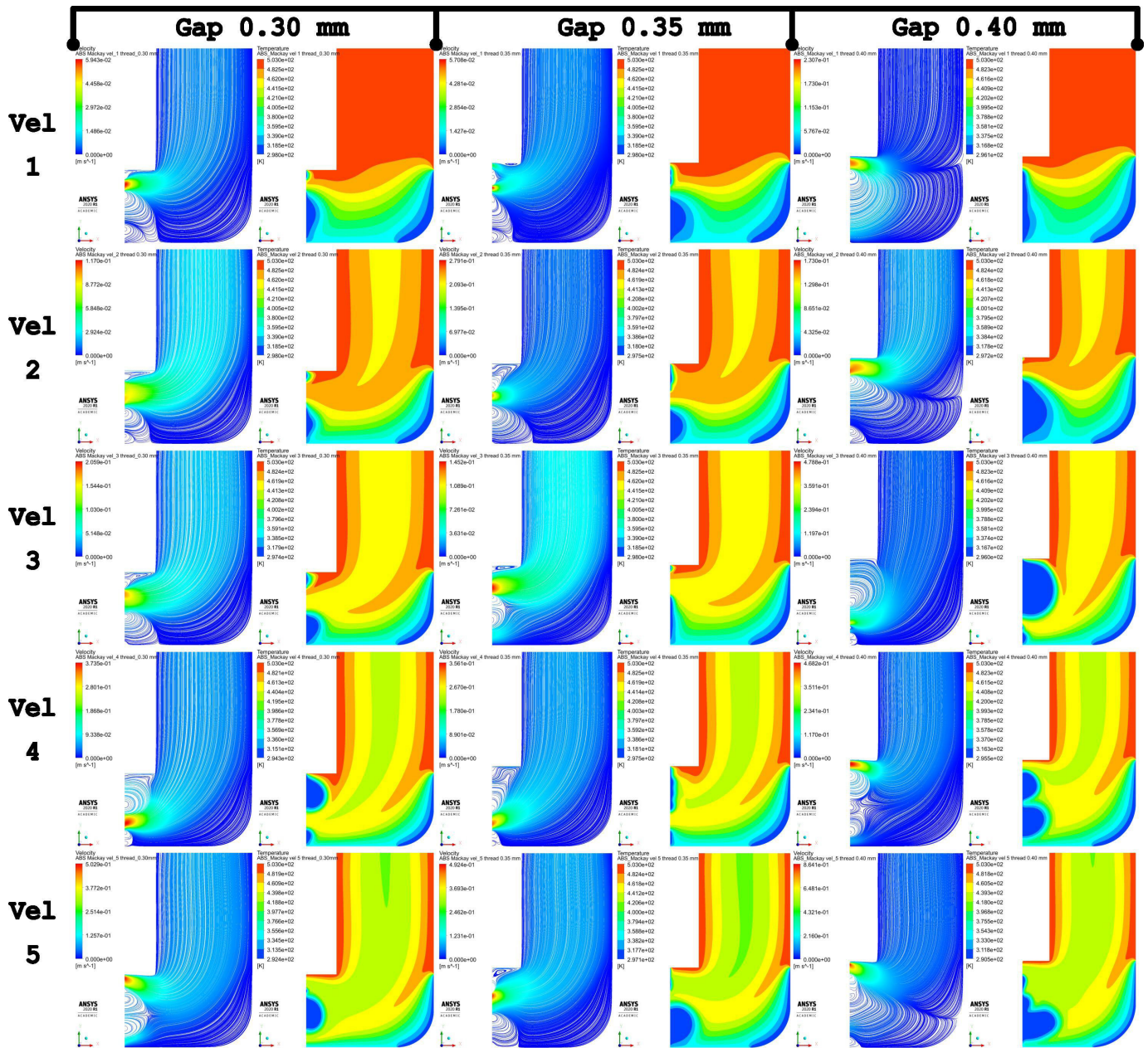


Fig. 7. Simulations using the velocities and gaps previously proposed, ABS Mackay

decreases abruptly in a short range of diameter the temperature changes as well, but when the velocity decreases at longer range of diameter the temperature changes less, compared to the other velocities (see Fig. 11).

In Figure 12 the velocity starts around 0 while the temperature increases, but when the velocity increases the temperature reaches and overshoot which lowers depending on the velocity changes.

Looking at Figs. 8 and 9 it is possible to observe that reaching the overshoot takes longer distance, in other words the lower the gap or diameter of the thread the

shorter the distance is needed to achieve the overshoot in the temperature values. In Figs. 10, 11 and 12 it can be seen that higher velocities are achieved while the gap is lowered, also when the feeding velocity is increased the velocity field increase as well. This can be correlated with the Figure 13, that shows how high shear rates are presented when the gap is lowered from 0.40 mm to 0.35 mm and then to 0.30 mm. and the feeding velocity is increased, so higher shear rates mean different temperatures and velocity fields. Figure 13 was obtained using Equation 2.

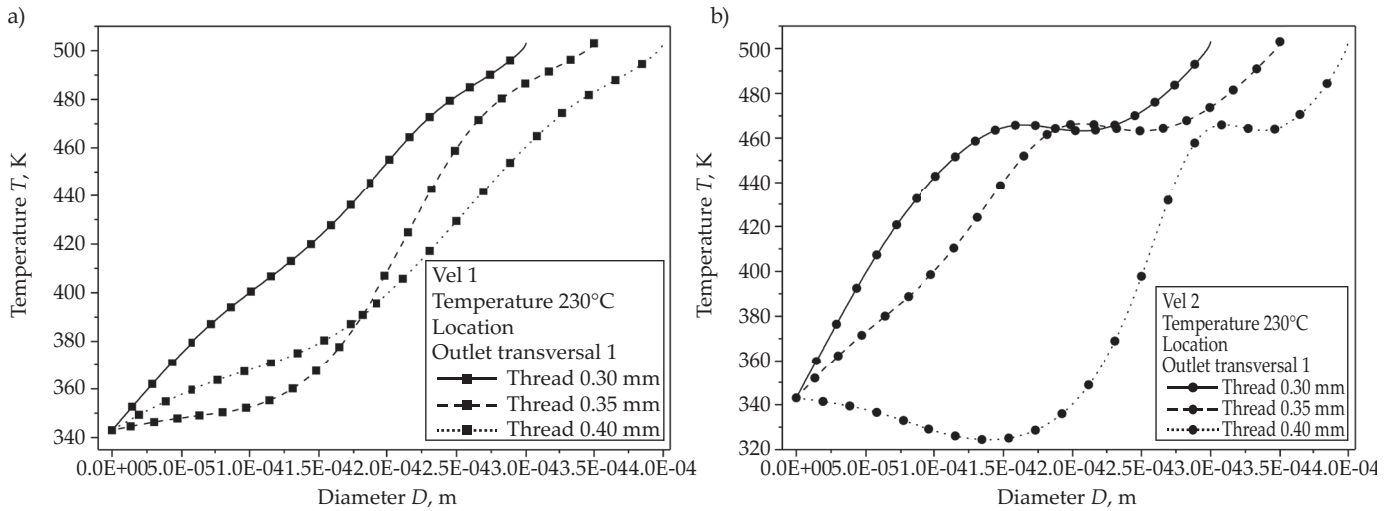


Fig. 8. The effect of velocity 1 (a) and 2 (b) and gap diameter on the temperature

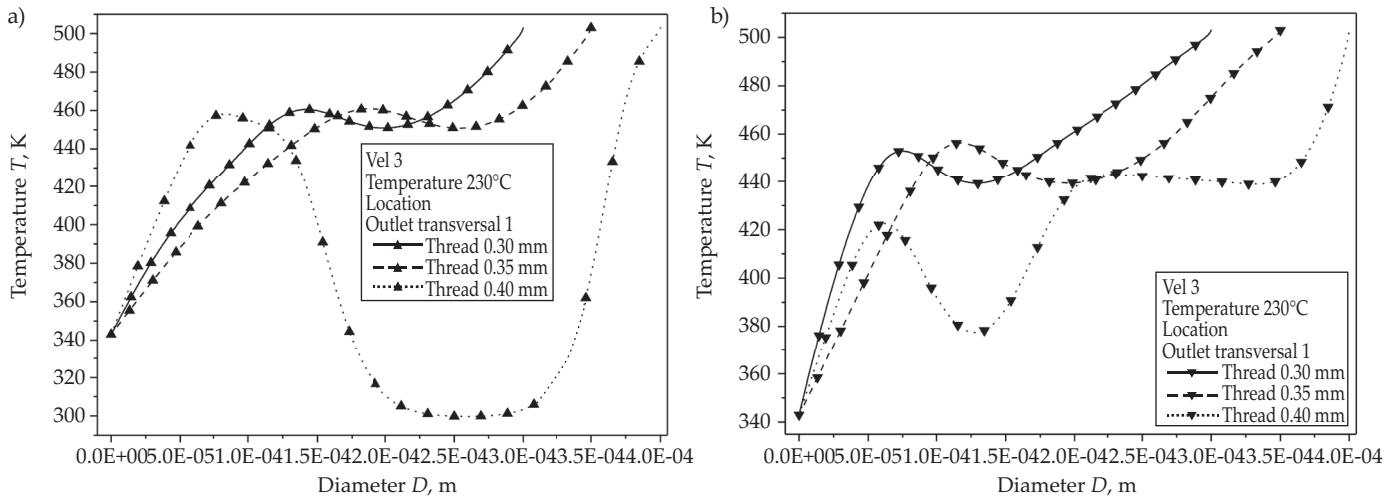


Fig. 9. The temperature behavior for printing velocity 3 (a) and 4 (b)

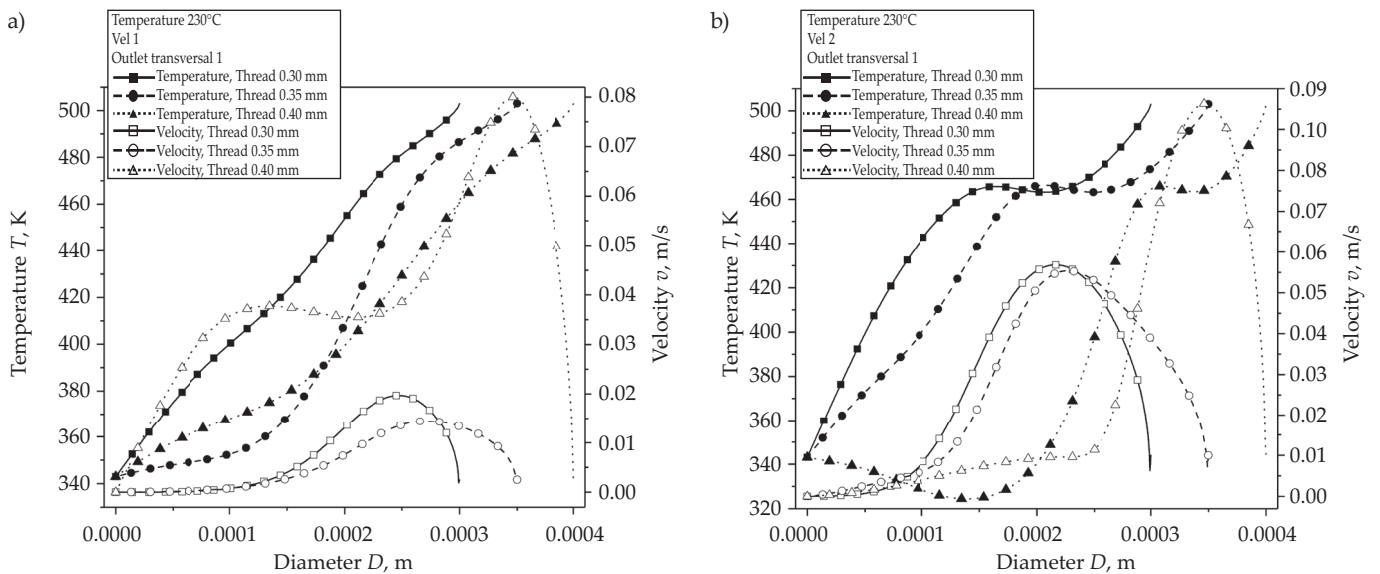


Fig. 10. Relation of the velocity and temperature at velocity 1 (a) and 2 (b)

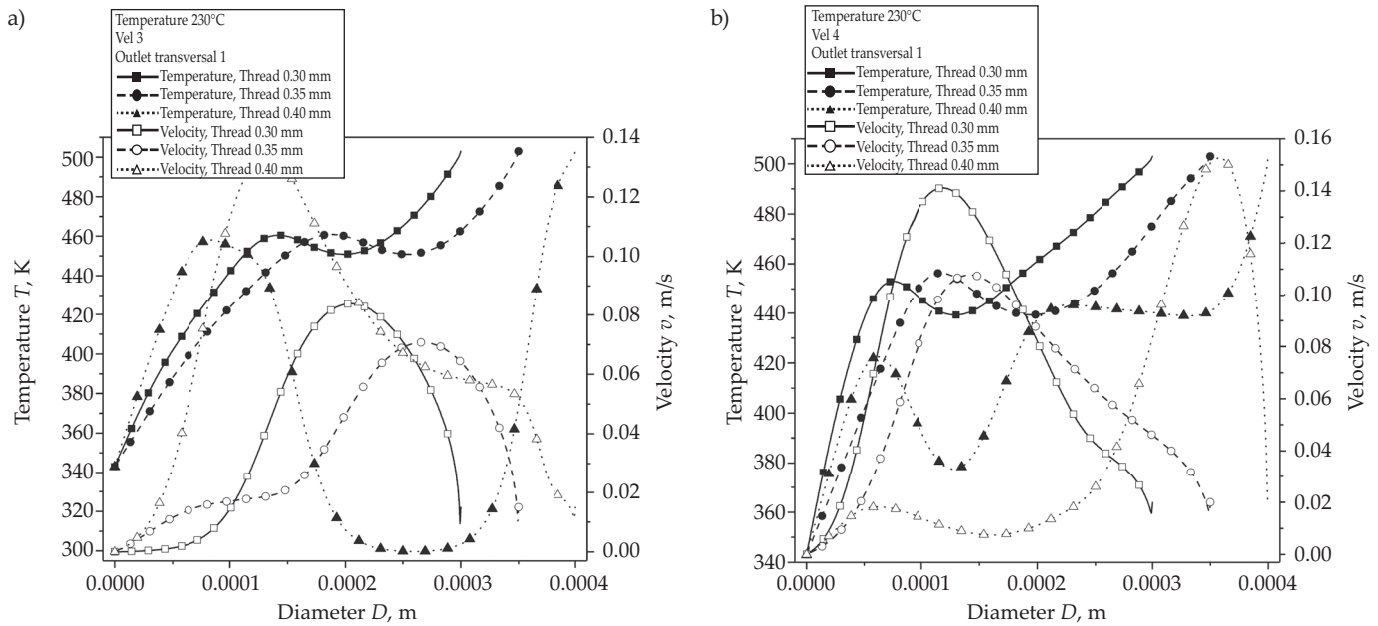


Fig. 11. Relation of the velocity and temperature at velocity 3 (a) and 4 (b)

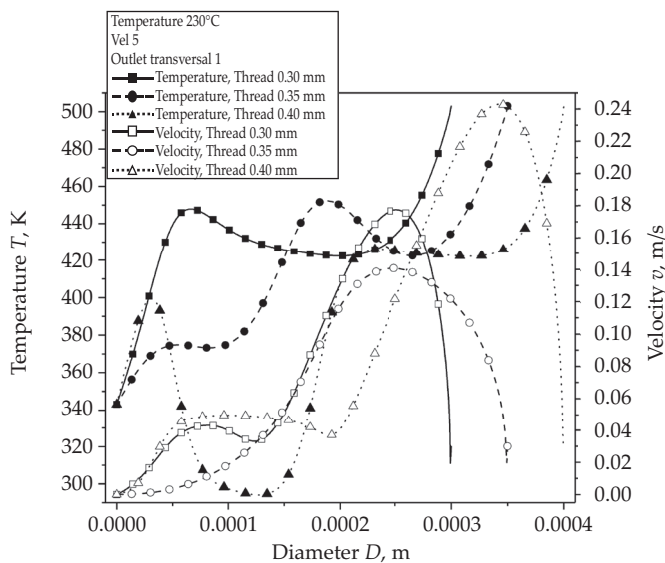


Fig. 12. Relation of the velocity and temperature at velocity 5

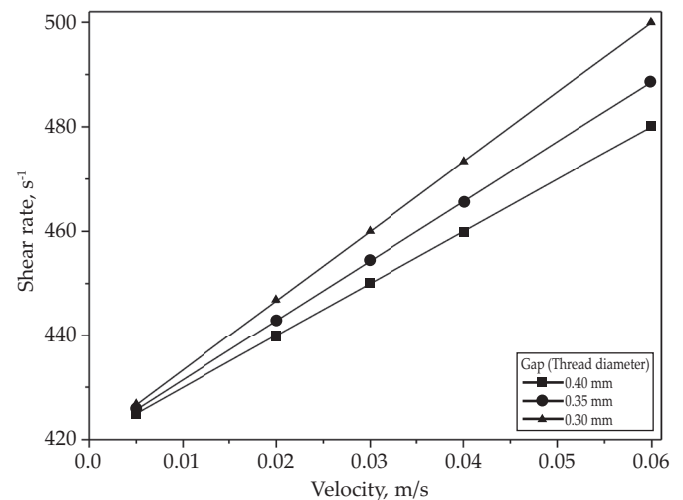


Fig. 13. Shear rate while the gap changes along with feeding velocity, data obtained using Equation 2

CONCLUSIONS

It was observed that gap or thread diameter have a great impact on the thread temperature and velocity at nozzle exit. While the gap decreases the velocity changes. When the gap is 0.30 mm, velocity 1 and 2 are the most suitable for printing. When the gap increases to 0.35 mm the velocity 3 and 4 are the more suitable. When the gap diameter is 0.4 mm the velocity 5 seems to fit for printing. It means that for the smaller gap diameter the lower printing velocity is needed.

ACKNOWLEDGEMENT

The authors are indebted to DGAPA U.N.A.M., for financial support through project No. PAPIIT IV100320.

REFERENCES

- [1] Turner B.N., Gold S.A.: *Rapid Prototyping Journal* **2015**, 21(3), 250. <https://doi.org/10.1108/RPJ-02-2013-0017>
- [2] Turner B.N., Strong R., Gold S.A.: *Rapid Prototyping Journal* **2015**, 20(3), 192. <https://doi.org/RPJ-01-2013-0012>
- [3] Zhou Y., Nyberg T., Xiong G., Liu D.: "Temperature Analysis in the Fused Deposition Modeling Process," in 3rd International Conference on Information Science and Control Engineering (ICISCE), 2016, pp. 678–682. <https://doi.org/10.1109/ICISCE.2016.150>
- [4] Yardimci M.A., Hattori T., Gucerli S.I., Danforth S.C.,

- “Thermal Analysis of Fused Deposition” in “Solid freeform fabrication”, University of Texas, Austin, 1997, vol. 8th, p. 10.
- [5] Wang Z., Smith D.E.: *Journal of Composites Science* **2018**, 2(1), 10.
<https://doi.org/10.3390/jcs2010010>
- [6] Ramanath H.S., Chua C.K., Leong K.F., Shah K.D.: *Journal of Materials Science: Materials in Medicine* **2008**, 19(7), 2541.
<https://doi.org/10.1007/s10856-007-3203-6>
- [7] Mostafa N., Syed H.M., Igor S., Andrew G.: *Tsinghua Science And Technology* **2009**, 14(S1), 29.
[https://doi.org/10.1016/S1007-0214\(09\)70063-X](https://doi.org/10.1016/S1007-0214(09)70063-X)
- [8] Papon E.A., Haque A., Sharif M.: “Effect of Nozzle Geometry on Melt Flow Simulation and Structural Property of Thermoplastic Nanocomposites in Fused Deposition Modeling,” Oct. 2017.
<https://doi.org/10.12783/asc2017/15339>
- [9] Heij W.J.: “Feed velocity feedback for high speed fused deposition modelling machines,” Master thesis, Biomedical Engineering, TU Delft, TU Delft Netherlands, 2016.
- [10] Bellini A.: “Fused deposition of ceramics: a comprehensive experimental, analytical and computational study of material behavior, fabrication process and equipment design”, iDEA: Drexel Libraries E-Repository And Archives,” Materials Engineering, Drexel University, Drexel University, 2002.
- [11] Mackay M.E., Swain Z.R., Banbury C.R. *et al.*: *Journal of Rheology* **2017**, 61(2), 229.
<https://doi.org/10.1122/1.4973852>
- [12] Geng P., Zhao J., Wu W. *et al.*: *Journal of Manufacturing Processes* **2019**, 37, 266.
<https://doi.org/10.1016/j.jmapro.2018.11.023>
- [13] Clasen C., Gearing B.P., McKinley G.H.: *Journal of Rheology* **2006**, 50(6), 883.
<https://doi.org/10.1122/1.2357190>
- [14] Baik S.J., Moldenaers P., Clasen C.: *Review of Scientific Instruments* **2011**, 82(3), 035121.
<https://doi.org/10.1063/1.3571297>

Received 18 III 2022.